

Symmetry breaking Rayleigh-Taylor instability in a two-component Bose-Einstein condensate

Tsuyoshi Kadokura,¹ Tomohiko Aoi,¹ Kazuki Sasaki,¹ Tetsuo Kishimoto,^{1,2,3} and Hiroki Saito¹

¹*Department of Engineering Science, University of Electro-Communications, Tokyo 182-8585, Japan*

²*Center for Frontier Science and Engineering, University of Electro-Communications, Tokyo 182-8585, Japan*

³*PRESTO, Japan Science and Technology Agency (JST), Saitama 332-0012, Japan*

(Dated: June 15, 2021)

The interfacial instability and subsequent dynamics in a phase-separated two-component Bose-Einstein condensate with rotation symmetry are studied. When the interatomic interaction or the trap frequency is changed, the Rayleigh-Taylor instability breaks the rotation symmetry of the interface, which is subsequently deformed into nonlinear patterns including mushroom shapes.

PACS numbers: 03.75.Mn, 67.85.De, 67.85.Fg, 47.20.Ma

I. INTRODUCTION

The Rayleigh-Taylor instability [1–4] (RTI) is an instability of an interface between two fluids in a metastable state. For instance, when a layer of a heavier fluid is laid on a lighter fluid, the system is energetically unfavorable and the two fluids tend to exchange their positions. However, if the two fluids are immiscible and their interface is flat, the exchange cannot occur without breaking the translation symmetry of the interface. Once an infinitesimal modulation arises on the interface, it exponentially grows due to the RTI, and the interface develops into complicated patterns such as a mushroom-shaped pattern. This kind of phenomena is found through nature in a wide scale ranging from laboratory to astronomical scales [5].

Recently, the RTI was predicted to be observed in a two-component Bose-Einstein condensate (BEC) [6, 7]. In Ref. [6], a two-component BEC trapped in a tight pancake-shaped trap is considered, in which the two components separate into two semicircular shapes in the trap. When an external force is applied to each component in the direction to the other component, the RTI sets in and the interface deforms into a mushroom-shaped pattern. In Ref. [7], the initial state of a two-component BEC forms a domain structure in the axial direction of a cigar-shaped trap. The interaction between atoms in one component is then increased, and the RTI arises at the domain wall.

The RTI is a symmetry breaking phenomenon, that is, even when the interface has symmetry (e.g. the translation symmetry of a flat interface) an infinitesimal modulation grows exponentially and the symmetry is spontaneously broken. However, in the above mentioned studies in Refs. [6, 7], the symmetry breaking cannot be observed explicitly, since the relevant symmetry is broken from the initial state: the interfaces have edges or rims and have no translation symmetry. The inhomogeneous interfaces of the initial state strongly affects the deformation dynamics of the interfaces, obscuring the symmetry breaking nature of the RTI.

In this paper, we propose a system to observe the sym-

metry breaking RTI for a trapped two-component BEC. We consider a two-component BEC with rotation symmetry, in which the two components separate radially and a “bubble” of inner component is surrounded by a shell of outer component. The interface between the two components has a spherical shape for an isotropic trap and a circular shape for a quasi-2D axisymmetric trap. If we change a parameter in such a way that the inner component tends to go out of the outer shell component, the RTI breaks the rotation symmetry of the interface and the spherical or circular interface is deformed into various patterns. The symmetry breaking RTI can thus be realized in a trapped BEC. The RTI that breaks rotation symmetry occurs in a variety of systems, such as supernova explosion [9], imploding targets in inertial-confinement fusion [10], and collapsing cavitation bubbles [11, 12].

This paper is organized as follows. Section II provides a formulation of the problem and Sec. III shows numerical results. Section III A demonstrates the symmetry-breaking RTI and subsequent dynamics for an axisymmetric oblate system. Section III B shows dynamics for an isotropic trap and performs Bogoliubov analysis. Section III C examines oscillation of interaction. Section IV gives conclusions to this study.

II. FORMULATION OF THE PROBLEM

We consider a mixture of two kinds of bosonic atoms with mass m_1 and m_2 confined in trapping potential V_1 and V_2 , respectively. The Hamiltonian for the system is given by

$$\hat{H} = \sum_{j=1}^2 \int d\mathbf{r} \hat{\psi}_j^\dagger \left(-\frac{\hbar^2}{2m_j} \nabla^2 + V_j \right) \hat{\psi}_j + \sum_{j,j'} \int d\mathbf{r} d\mathbf{r}' \hat{\psi}_j^\dagger(\mathbf{r}) \hat{\psi}_{j'}^\dagger(\mathbf{r}') U_{jj'}(\mathbf{r} - \mathbf{r}') \hat{\psi}_{j'}(\mathbf{r}') \hat{\psi}_j(\mathbf{r}), \quad (1)$$

where $\hat{\psi}_j$ is the bosonic field operator for component j and $U_{jj'}$ is the interaction between atoms of components j and j' . In the mean-field theory, we assume that the atoms in each component occupy the same wave function ψ_j and that the interaction potential is reduced to the Fermi pseudopotential,

$$U_{jj'}(\mathbf{r} - \mathbf{r}') = 2\pi\hbar^2 a_{jj'} (m_j^{-1} + m_{j'}^{-1}) \delta(\mathbf{r} - \mathbf{r}') \equiv g_{jj'} \delta(\mathbf{r} - \mathbf{r}'), \quad (2)$$

where $a_{jj'}$ is the s -wave scattering length between the atoms in components j and j' . The system is thus described by the two-component Gross-Pitaevskii (GP) equation ($j \neq j'$),

$$i\hbar \frac{\partial \psi_j}{\partial t} = \left(-\frac{\hbar^2}{2m_j} \nabla^2 + V_j + g_{jj} |\psi_j|^2 + g_{jj'} |\psi_{j'}|^2 \right) \psi_j. \quad (3)$$

The macroscopic wave functions are normalized as $\int |\psi_j|^2 d\mathbf{r} = N_j$ with N_j being the number of atoms in component j . The two components are miscible for $g_{11}g_{22} > g_{12}^2$ and immiscible for $g_{11}g_{22} < g_{12}^2$.

We solve the 3D GP equation (3) numerically using the pseudospectral method [8]. The initial state is the ground state prepared by the imaginary-time propagation method, in which i on the left-hand side of Eq. (3) is replaced by -1 . We then add a small noise to the initial state as a seed that triggers the RTI. The dynamics do not depend on the initial noise qualitatively.

In the following calculations, we assume a dual-species BEC with ^{85}Rb and ^{87}Rb , where the $|f=2, m_f=-2\rangle$ state of ^{85}Rb is component 1 and the $|f=1, m_f=-1\rangle$ state of ^{87}Rb is component 2. This system has been realized by the JILA group [13], in which controlled phase separation was observed by changing the s -wave scattering length a_{11} of ^{85}Rb using a magnetic-field Feshbach resonance, which is variable in the range $a_{11} = 50\text{-}900a_B$ with a_B being the Bohr radius. Since $a_{22} = 99a_B$ and $a_{12} = 213a_B$, the condition for the phase separation is satisfied for $a_{11} < 458a_B$.

III. NUMERICAL RESULTS

A. Rayleigh-Taylor instability in axisymmetric oblate systems

We first demonstrate the dynamics for an axisymmetric oblate trap, $V_j = m_j[\omega_\perp^2(x^2 + y^2) + \omega_z^2 z^2]/2$, where $\omega_z \gg \omega_\perp$. We assume that the gravitational sag is compensated and the two components share a common trap center. Figure 1 shows the time evolution of the density and phase profiles of the system, obtained by solving the 3D GP equation (3). The initial state is the ground state for $a_{11} = 80a_B$ and $N_1 = N_2$, which has the axisymmetric circular interface between the two components [Fig. 1 (a)]. The repulsive interaction of component 1 (inner) is then gradually increased and when it exceeds that of

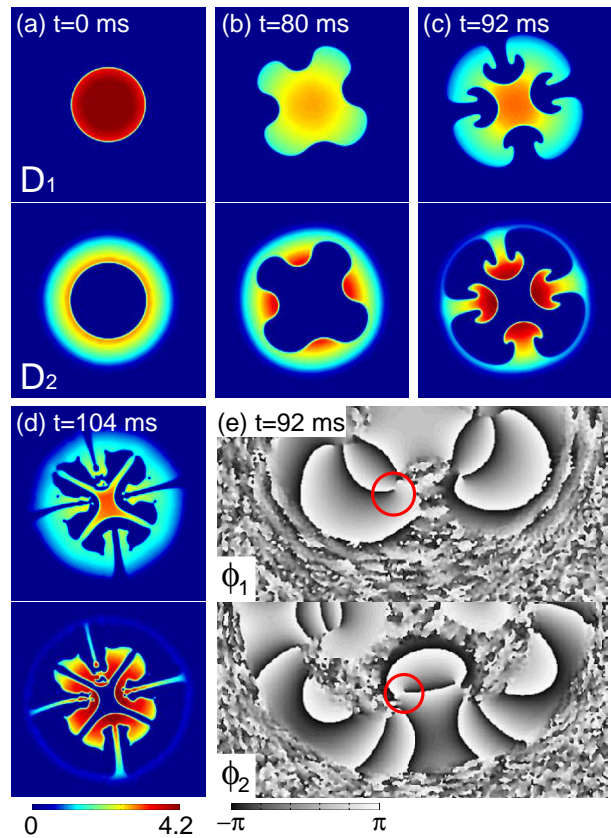


FIG. 1: (Color online) (a)-(d) Dynamics of the column density profiles $D_1 = \int |\psi_1|^2 dz$ (upper panels) and $D_2 = \int |\psi_2|^2 dz$ (lower panels) in an axisymmetric trap with $(\omega_\perp, \omega_z) = 2\pi \times (25, 1250)$ Hz. The scattering length a_{11} is linearly increased from $80a_B$ to $240a_B$ between $t = 0$ and $t = 40$ ms, and after that a_{11} is fixed to $240a_B$. The numbers of atoms are $N_1 = N_2 = 10^5$. The unit of the column density is 10^{12} cm^{-2} . (e) Cross-sectional phase profile $\phi_j = \arg[\psi_j(z=0)]$ of the lower half region of (c). The circles in (e) indicate examples of quantized vortices created under the caps of the mushrooms. The field of view is $65.4 \times 65.4 \mu\text{m}$ in (a)-(d) and $65.4 \times 32.7 \mu\text{m}$ in (e).

component 2 (outer) the system becomes metastable, i.e., the state in which component 1 surrounds component 2 becomes energetically favorable. At $t \simeq 80$ ms, the axisymmetry of the system is broken and the interface is modulated due to the RTI [Fig. 1 (b)]. The modulation of the interface subsequently grows to become a four-fold mushroom shape [Fig. 1 (c)]. Quantized vortices are generated under the caps of the mushrooms in both components [circles in Fig. 1 (e)]. When the tops of the mushrooms reach the edge or the center of the system, a highly nonlinear pattern is observed [Fig. 1 (d)]. The n -fold mushroom shapes with $n \neq 4$ are also observed, where n is larger for a larger final value of a_{11} .

The dynamics also depends on the ratio between the numbers of atoms N_2/N_1 . Figure 2 shows the dynamics for $N_2/N_1 = 1/9$. After the repulsive interaction of component 1 is increased, the RTI causes modulation at the

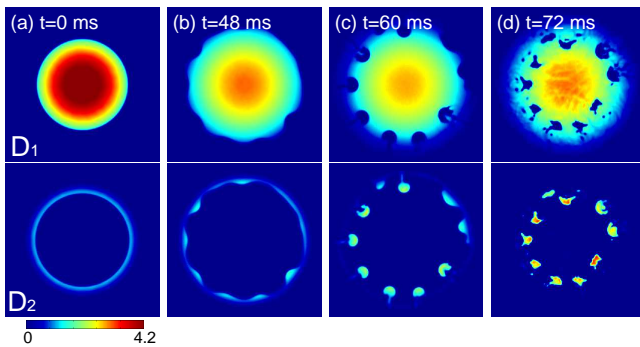


FIG. 2: (Color online) Dynamics of the column density profiles D_1 and D_2 for $N_1 = 1.8 \times 10^5$ and $N_2 = 2 \times 10^4$. Other parameters are the same as those in Fig. 1.

interface [Fig. 2 (b)]. Since N_2 is small, the ring of component 2 splits into droplets, which enter the component 1 forming small mushrooms [Fig. 2 (c)]. The droplets of component 2 then go towards the center and gather, where their complicated shapes are similar to air bubbles rising in water.

B. Rayleigh-Taylor instability in an isotropic system

Next we consider a system confined in an isotropic trap given by $V_j = m_j \omega_j^2 r^2 / 2$ with $r^2 = x^2 + y^2 + z^2$. The initial state is the ground state for $a_{11} = 200a_B$ and $\omega_1 = \omega_2$, in which component 2 with a spherical shape is surrounded by a shell of component 1 [Fig. 3 (a)]. The trap frequency ω_1 of component 1 is then increased gradually. The outer component is pushed inward by the increase in the trap frequency and the RTI is induced at the spherical interface. At $t \simeq 36$ ms, the RTI breaks the rotation symmetry and the spherical interface is modulated [Figs. 3 (b) and 3 (d)]. The interface is then deformed into a “mushroom ball” [Fig. 3 (e)].

The unstable modes of the interface is estimated by a simple analysis. We assume inviscid, incompressible, and irrotational fluids and component 2 of a spherical bubble with radius R is surrounded by component 1. The excitation frequency Ω of the interfacial mode proportional to the spherical harmonics $Y_l^m(\theta, \phi)$ is given by [14]

$$\Omega^2 = \frac{l(l+1)}{R[lm_1n_1 + (l+1)m_2n_2]} \times \left[n_2f_2 - n_1f_1 + \frac{(l-1)(l+2)}{R^2}\sigma \right], \quad (4)$$

where n_j is the atomic density, f_j is the external force acting on an atom at the interface, and σ is the interfacial tension coefficient. If Ω is pure imaginary, i.e., the right-hand side of Eq. (4) is negative, the mode is dynamically unstable. Using the expression of σ for a two-component BEC derived in Ref. [15] and $f_j = m_j \omega_j^2 R$, we find that

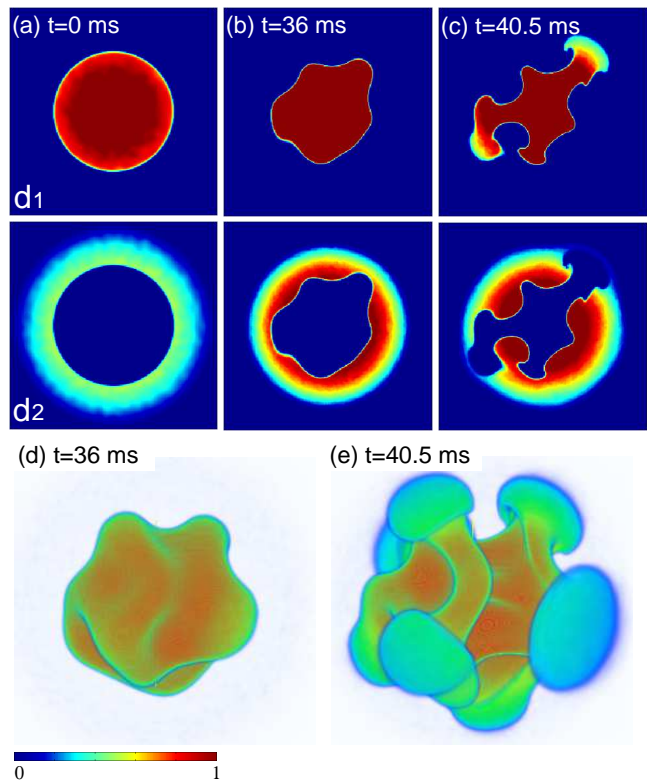


FIG. 3: (Color online) (a)-(c) Dynamics of the cross-sectional density profiles $d_1 = |\psi_1(z=0)|^2$ and $d_2 = |\psi_2(z=0)|^2$ of components 1 and 2 and (d), (e) the isodensity surfaces of component 1 in an isotropic trap with frequency $\omega_1(t=0) = \omega_2 = 2\pi \times 33.3$ Hz. The trap frequency ω_1 is increased such that ω_1^2 is linearly increased from $(\omega_1/\omega_2)^2 = 1$ to 3 between $t = 0$ and $t = 30$ ms, and after that $(\omega_1/\omega_2)^2$ is fixed to 3. The scattering length of component 1 is $a_{11} = 200a_B$ and the numbers of atoms are $N_1 = N_2 = 5.2 \times 10^6$. The unit of the density is $3.0 \times 10^{14} \text{ cm}^{-3}$. The field of view of each panel is $56.6 \times 56.6 \mu\text{m}$.

the modes for $1 \leq l \leq 7$ are unstable for the parameters in Fig. 3, which seems to be consistent with the interfacial pattern shown in Fig. 3. However, this estimation is only qualitative since the compressibility and the inhomogeneous density distribution of a BEC are not taken into account.

From Eq. (4), we find that the RTI is induced by an increase in ρ_1 or f_1 , or by a decrease in ρ_2 or f_2 . The density ρ_j depends on the interaction: an increase (decrease) in a_{jj} expands (contracts) component j , which decreases (increases) ρ_j . The force f_j acting on each component can be controlled, if the external trapping potential for each component can be controlled independently. The RTI can thus be induced in several ways: for example, (i) an increase in the scattering length of inner component, (ii) a decrease in the trap frequency for inner component, (iii) a decrease in the scattering length of outer component, and (iv) an increase in the trap frequency for outer component. The dynamics shown in Figs. 1 and 3 correspond to (i) and (iv), respectively. We have numer-

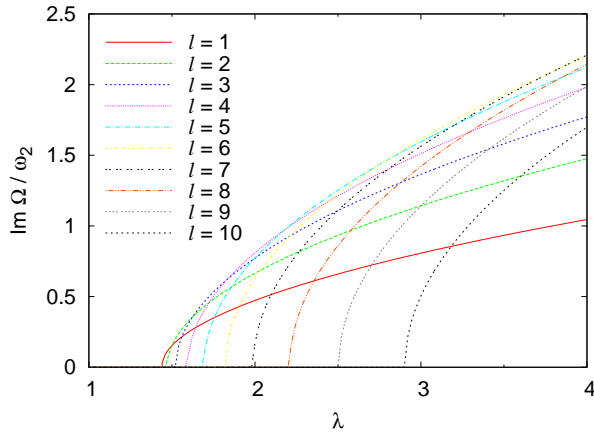


FIG. 4: (Color online) Imaginary part of the Bogoliubov excitation frequency, $\text{Im } \Omega$, as a function of $\lambda \equiv (\omega_1/\omega_2)^2$. The parameters are the same as those in Fig. 3. The modes for $l \leq 8$ are plotted, where l is defined in Eq. (5).

ically confirmed that the RTI can be observed by all the methods (i)-(iv) for both axisymmetric oblate trap and isotropic trap.

For more precise understanding of the instability, we perform the Bogoliubov analysis for an isotropic trap. We expand the GP equation (3) up to the first order of the deviation $\delta\psi_j(\mathbf{r})$ from the initial stationary state $\Psi_j(r)$ with spherical symmetry. The excitation mode of the form

$$\delta\psi_j = u_j(r)Y_l^m(\theta, \phi) + v_j^*(r)Y_l^{m*}(\theta, \phi) \quad (5)$$

obeys the Bogoliubov-de Gennes equation ($j \neq j'$)

$$(K_{jl} + V_j - \mu_j + 2g_{jj}\Psi_j^2 + g_{jj'}\Psi_{j'}^2)u_j + g_{jj}\Psi_j^2v_j + g_{jj'}\Psi_j\Psi_{j'}(u_{j'} + v_{j'}) = \hbar\Omega u_j, \quad (6a)$$

$$(K_{jl} + V_j - \mu_j + 2g_{jj}\Psi_j^2 + g_{jj'}\Psi_{j'}^2)v_j + g_{jj}\Psi_j^2u_j + g_{jj'}\Psi_j\Psi_{j'}(u_{j'} + v_{j'}) = -\hbar\Omega v_j, \quad (6b)$$

where μ_j is the chemical potential and

$$K_{jl} = -\frac{\hbar^2}{2m_j} \left[\frac{d^2}{dr^2} + \frac{2}{r} \frac{d}{dr} - \frac{l(l+1)}{r^2} \right]. \quad (7)$$

The stationary wave function Ψ_j is assumed to be real without loss of generality. We numerically diagonalize Eq. (6) to study the stability of the system. If there is a complex frequency Ω , the corresponding mode grows exponentially and the system is dynamically unstable. Figure 4 shows the imaginary part of the Bogoliubov excitation frequency, $\text{Im } \Omega$, as a function of $(\omega_1/\omega_2)^2$. The critical value of $(\omega_1/\omega_2)^2$ above which $\text{Im } \Omega$ rises increases with an increase in l , and above this critical value of $(\omega_1/\omega_2)^2$, $\text{Im } \Omega$ monotonically increases. At $(\omega_1/\omega_2)^2 = 3$, which corresponds to Fig. 3, $\text{Im } \Omega$ for the $l = 5-7$ modes are comparably large and these modes dominate the unstable dynamics.

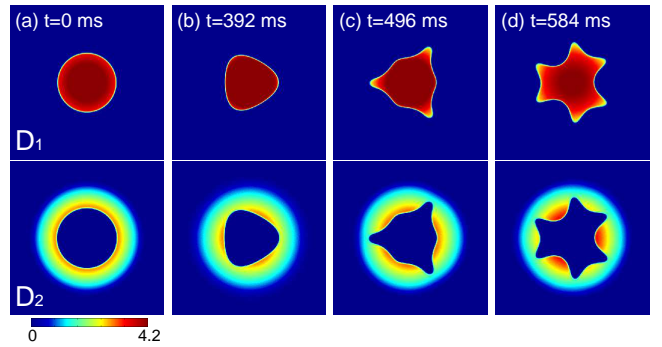


FIG. 5: (Color online) Dynamics of the column density profiles D_1 and D_2 , in which a_{11} is oscillated as in Eq. (8) with $a_0 = 80a_B$, $A = 0.4$, and $\omega_a = 2\pi \times 30$ Hz. Other parameters are the same as those in Fig. 1. The unit of the column density is 10^{12} cm^{-2} . The field of view of each panel is $65.4 \times 65.4 \mu\text{m}$.

C. Oscillation of the interaction

We demonstrate another symmetry breaking dynamics that is not due to the RTI. We return to the tight pancake-shaped trap used in Fig. 1, and study the dynamics for an oscillating interaction. The scattering length of component 1 is oscillated as

$$a_{11} = a_0(1 + A \sin \omega_a t), \quad (8)$$

where a_0 , A , and ω_a are constants. Figure 5 shows the dynamics of the column density profile. By the oscillating repulsive interaction of the inner component, the circular interface undergoes breathing oscillation. The axisymmetry of the interface is then spontaneously broken [Fig. 5 (b)], which is understood as the parametric amplification of an interface mode. The interface subsequently exhibits various patterns [Figs. 5 (b) and 5 (c)]. A variety of patterns can be observed depending on the parameters in Eq. (8) (data not shown).

IV. CONCLUSIONS

In conclusion, we have investigated the interfacial instabilities and subsequent dynamics in phase-separated two-component BECs. Since the initial state has rotation symmetry, the symmetry breaking nature of the RTI can specifically be observed in this system. We have demonstrated the RTI and ensuing dynamics for an axisymmetric oblate trap (Figs. 1 and 2) and an isotropic trap (Fig. 3), and the mushroom-shaped patterns are observed for both systems breaking the rotation symmetry. We performed the Bogoliubov analysis for the isotropic system and obtained the unstable spectrum (Fig. 4). We also examined the dynamics for oscillating interaction and found that the axisymmetry is spontaneously broken and nonlinear patterns emerge (Fig. 5).

In view of the recent development in the control of two-component BECs [13, 16, 17], we expect that not only the phenomena predicted in the present paper but also other theoretical predictions [18–23] concerning the interfacial instabilities in two-component BECs will be realized in experiments in the near future.

Acknowledgments

This work was supported by Grants-in-Aid for Scientific Research (No. 22340116, No. 23540464, and No.

23740307) from the Ministry of Education, Culture, Sports, Science and Technology of Japan, and Japan Society for the Promotion of Science. T. Kishimoto thanks for Special Coordination Funds for Promoting Science and Technology (Highly Talented Young Researcher) from Japan Science and Technology Agency.

-
- [1] Lord Rayleigh, Proc. London Math. Soc. **14**, 170 (1883).
 - [2] G. I. Taylor, Proc. Roy. Soc. London Ser. A **201**, 192 (1950).
 - [3] D. J. Lewis, Proc. Roy. Soc. London Ser. A **202**, 81 (1950).
 - [4] For example, see, S. Chandrasekhar, *Hydrodynamic and Hydromagnetic Stability* (Clarendon Press, Oxford, 1961), Chapter 10.
 - [5] W. Schmidt, Nature Phys. **2**, 505 (2006).
 - [6] K. Sasaki, N. Suzuki, D. Akamatsu, and H. Saito, Phys. Rev. A **80**, 063611 (2009).
 - [7] S. Gautam and D. Angom, Phys. Rev. A **81**, 053616 (2010).
 - [8] W. H. Press, S. A. Teukolsky, W. T. Vetterling, B. P. Flannery, *Numerical Recipes*, 3rd ed, Sec. 20.7 (Cambridge Univ. Press, Cambridge, 2007).
 - [9] A. Burrows, Nature (London) **403**, 727 (2000).
 - [10] H. Sakagami and K. Nishihara, Phys. Rev. Lett. **65**, 432 (1990).
 - [11] M. S. Plesset, J. Appl. Phys. **25**, 96 (1954).
 - [12] M. P. Brenner, D. Lohse, and T. F. Dupont, Phys. Rev. Lett. **75**, 954 (1995).
 - [13] S. B. Papp, J. M. Pino, and C. E. Wieman, Phys. Rev. Lett. **101**, 040402 (2008).
 - [14] H. Lamb, *Hydrodynamics*, 6th ed, Sec. 275 (Dover, New York, 1945).
 - [15] B. Van Schaeybroeck, Phys. Rev. A **78**, 023624 (2008); **80**, 065601 (2009).
 - [16] K. M. Mertes, J. W. Merrill, R. Carretero-González, D. J. Frantzeskakis, P. G. Kevrekidis, and D. S. Hall, Phys. Rev. Lett. **99**, 190402 (2007).
 - [17] S. Tojo, Y. Taguchi, Y. Masuyama, T. Hayashi, H. Saito, and T. Hirano, Phys. Rev. A **82**, 033609 (2010).
 - [18] H. Saito, Y. Kawaguchi, and M. Ueda, Phys. Rev. Lett. **102**, 230403 (2009).
 - [19] H. Takeuchi, N. Suzuki, K. Kasamatsu, H. Saito, and M. Tsubota, Phys. Rev. B **81**, 094517 (2010).
 - [20] N. Suzuki, H. Takeuchi, K. Kasamatsu, M. Tsubota, and H. Saito, Phys. Rev. A **82**, 063604 (2010).
 - [21] A. Bezett, V. Bychkov, E. Lundh, D. Kobayakov, and M. Marklund, Phys. Rev. A **82**, 043608 (2010).
 - [22] D. Kobayakov, V. Bychkov, E. Lundh, A. Bezett, V. Akkerman, and M. Marklund, Phys. Rev. A **83**, 043623 (2011).
 - [23] K. Sasaki, N. Suzuki, and H. Saito, Phys. Rev. A **83**, 053606 (2011).